RSC Advances

This is an *Accepted Manuscript*, which has been through the Royal Society of Chemistry peer review process and has been accepted for publication.
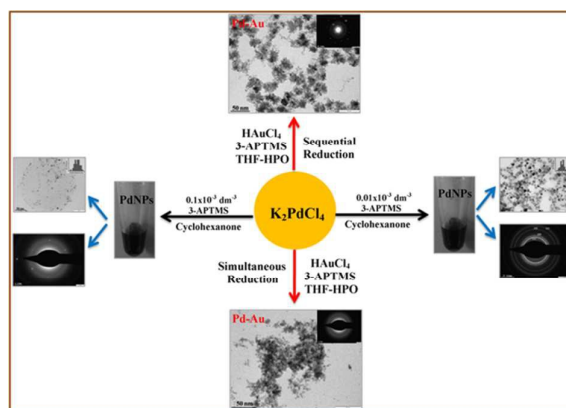
Accepted Manuscripts are published online shortly after acceptance, before technical editing, formatting and proof reading. Using this free service, authors can make their results available to the community, in citable form, before we publish the edited article. This *Accepted Manuscript* will be replaced by the edited, formatted and paginated article as soon as this is available.

You can find more information about *Accepted Manuscripts* in the **Information for Authors**.

Please note that technical editing may introduce minor changes to the text and/or graphics, which may alter content. The journal's standard **Terms & Conditions** and the **Ethical guidelines** still apply. In no event shall the Royal Society of Chemistry be held responsible for any errors or omissions in this *Accepted Manuscript* or any consequences arising from the use of any information it contains.

Table of Contents

ARTICLE TYPE

Controlled synthesis of Pd and Pd-Au nanoparticles: Effect of Organic amine and silanol groups on morphology and polycrystallinity of nanomaterials

Prem. C. Pandey*and Richa Singh

The synthesis of palladium (PdNPs) and its bimetallic (Pd-Au/Au-Pd) nanoparticles of controlled nanogeometry, polycrystallinity and functional ability is challenging task. We report a new process for metal nanoparticles synthesis meeting these requirements that incorporate the specific role of 10 organic amine and silanol functionalities with following major findings: (1) the concentrations of organic amine control the nanogeometry and functional ability of nanoparticles; (2) polycrystallinity of PdNPs tend to decrease as a function of silanol concentration justifying specific interaction of PdNPs and silanol group whereas AuNPs do not show such interaction; (3) transition in 15 microstructure from hexagonal nanogeometry to circular nanogeometry of palladium nanoparticles (PdNPs) in the presence of silanol group (4) initial reduction of palladium ions followed by reduction of gold ions during the synthesis of bimetallic nanoparticles results negligible interaction of silanol residue and PdNPs justifying an increase in polycrystallinity whereas 20 simultaneous reduction of the same enable decrease in polycrystallinity, (5) initial reduction of gold ions causes aggregation of same forming larger nanoparticles and reveals negligible interaction with silanol content under similar conditions, (6) the size of nanoparticles decreases with an increase in silanol concentration as a function of nanoparticle-silanol interaction. As 25 synthesized PdNPs shows peroxidase mimetic activity as a function of 3-APTMS concentration.

Introduction

The synthesis of palladium nanoparticles 30 (PdNPs) has received closer attention due to its remarkable applications in hydrogenation

reactions,[1-5] catalytic oxidation,[6-9] carbon–carbon bond formation[10-12] and electrochemical reactions in fuel cells.[13-15] Homogeneous dispersion of PdNPs meets the requirement of some of the applications however major technological needs require the presence of PdNPs in thin film formulation. Functionalization of PdNPs allows tailoring the specific properties in homogeneous or heterogeneous matrix through control over polycrystallinity, morphology and dispersibility. The use of organic amine as functional reagent has received greater attention due to stabilization of nanomaterials in homogeneous phase and simultaneously allowing the formation of biocompatible linkage.[16,17]

The use of 3-aminopropyltrimethoxysilane (3-APTMS) has been very well documented as potential stabilizer for noble metal nanoparticles.[18,19] Simultaneously, the use of same also enable the formation of nanostructured thin film of organically modified silicate (Ormosil) in the presence of another hydrophobic functional alkoxysilane precursors such as 3-glycidoxypropyltrimethoxysilane (GPTMS), 2-(3-epoxycyclohexyl) ethyltrimethoxysilane (ECETMS), trimethoxysilane (TMS) through sol-gel processing.[20-22] The ratio of hydrophilic (3-APTMS) and hydrophobic components play a vital role in casting thin film of nanostructured matrix for practical applications displaying measurable mass transfer and charge transfer dynamics. An increase in hydrophilic part allows

increasing the water wettability of ormosil film and reverse of the same tend to enable the formation of xerogel in shorter time. Nanostructured matrices could be manipulated in the presence of many active materials during sol-gel processing introducing desired reactivity in thin film. One of the potential needs during biocatalysis is the occurrence of reversible redox behaviour of membrane matrix resulting due to the encapsulation of redox mediator like ferrocene monocarboxylic acid (Fc-COOH) within ormosil thin film made from the suitable composition of hydrophobic and hydrophilic precursors. Two combinations of these precursors; e.g (1) GPTMS and TMS; (2) 3-APTMS and ECETMS; in appropriate ratio were used for thin film development encapsulating the Fc-COOH. The redox electrochemistry of ormosil-encapsulated Fc-COOH in both cases was found to display sluggish reversible electrochemistry mainly due to restricted mobility of ferrocenium ions within nanostructured network. In addition to that Fc-COOH loses its mediation capability required for designing mediated electrochemical sensors[23] under such condition. These findings directed to design ormosil film fulfilling the requirement of ferrocene-mediated bioelectrochemical sensing and the choice of electrocatalyst in combination with encapsulated mediator for facilitating electron transfer process became significant. Fortunately the interaction of palladium chloride (PdCl$_2$) and GPTMS while making ormosil film

with TMS has been recorded.[24,25] It was found that palladium chloride / tetrachlorpalladate (PdCl$_2$ /K$_2$PdCl$_4$) opens the epoxide ring of glycidoxy residue and in turn gets reduced into palladium followed by subsequent co-ordination within two glycidoxy residue.[24] The redox electrochemistry of the Fc-COOH when encapsulated within ormosil film made from palladium linked-GPTMS and TMS showed excellent reversible electrochemistry even better than that of the same recorded in homogeneous solution[24] and the resulting nanostructured thin film was efficient for catalyzing the re-generation of redox enzyme during mediated bioelectrochemical sensing. While resolving the reasons for excellent reversible redox electrochemical behaviour of ferrocene in such system, we found that trimethoxysilane (TMS) itself interact with PdCl$_2$ and results into the formation of Pd-Si linkage[24,26] and enable the formation of novel nanostructured domains in the presence of palladium-linked GPTMS justifying solid solution matrix for practical application of material in technological design. The results on the interaction of palladium chloride with GPTMS and TMS revealed following two major conclusions: (1) functionalized alkoxysilane acts as reducing agents for the reduction of metal ions; (2) as generated palladium nanoparticles show good affinity with silica matrix. Such remarkable conclusion has directed us to investigate synthesis of palladium nanoparticles involving the active role of 3-APTMS and other suitable organic functional group that precisely alter the hydrophilicity/hydrophobicity of nanomaterials. We report herein the use of 3-APTMS mediated synthesis of amphiphilic PdNPs, controlling polycrystallinity, morphology and dispersiblity of the same. Such amphiphilic PdNPs are liable for their use in either homogeneous dispersion in a variety of solvents or stabilization in silicate based matrices providing a promising way to benefit from the advantages of nanocrystalline dispersions for optical, catalytic, and electrochemical applications based thin film technology. The use of cyclohexanone and tetrahydrofuran hydroperoxide in combination of 3-APTMS during the synthesis of amphiphilic PdNPs are reported herein.

Experimental Section

Chemicals

3-aminopropyltrimethoxysilane (3-APTMS), potassium tetrachloropalladate (II) [K$_2$PdCl$_4$], tetrachloroauric acid (HAuCl$_4$) and o-dianisidine were obtained from Aldrich Chemical Co., India. Tetrahydrofuran (THF), cyclohexanone and hydrogen peroxide were obtained from Merck, India. Tetrahydrofuran hydroperoxide (THF-HPO) was synthesized by autoxidation of THF. All other chemical employed were of analytical grade.

Synthesis of Pd, Pd-Au and Au-Pd nanoparticles

3-APTMS and Cyclohexanone mediated synthesis of PdNPs.   PdNPs were synthesized using Cyclohexanone in absence and the presence of 3-APTMS. In absence of 3-APTMS 0.005 mol L^{-1} methanolic solution of K_2PdCl_4 was mixed with 1.9 mol L^{-1} cyclohexanone and allowed to stand for room temperature. PdNPs in the presence of 3-APTMS and cyclohexanone was made under two different conditions; (1) keeping the constant concentration of cyclohexanone while varying the concentration of 3-APTMS; (2) keeping the concentration of 3-APTMS constant while varying the concentration of cyclohexanone. The typical process for PdNPs synthesis following condition (1) involves the mixing of methanolic solution of metal salts, 3-APTMS and Cyclohexanone as shown in Table 1. Similarly the typical process for the synthesis of PdNPs following condition (2) involves mixing of 3-APTMS treated metal salt with variable concentration of cyclohexanone as shown in Table-2. A typical process for cyclohexanone and 3-APTMS mediated synthesis of PdNPs sol consisted of following steps: 50μL of 7 mM of K_2PdCl_4 solution in methanol was premixed with 10 μL of methanolic solution of 3-APTMS stirred for 2 min, followed by addition of cyclohexanone. The solution was kept undisturbed for 2 hrs. PdNPs sols of black color was obtained within <2hrs. The concentration of 3-APTMS, cyclohexanone and potassium tetrachloropalladate required for PdNPs sol formation are shown in Table-1 and Table-2.

Table 1 Characteristics of PdNPs sol as a function of 3-Aminopropyltrimethoxysilane (3-APTMS) concentration

S.No.	K_2PdCl_4 (mol dm^{-3})	3-APTMS (mol dm^{-3})	Cyclohexanone (mol dm^{-3})	PdNPs formation	Extent of Formation
1	0.005	0.001x10^{-3}	1.9	Black	+++
2	0.005	0.01x10^{-3}	1.9	Black	++++
3	0.005	0.1x10^{-3}	1.9	Black	++++
4	0.005	1x10^{-3}	1.9	Light Yellow	-
5	0.005	3x10^{-3}	1.9	Light Yellow	-
6	0.005	5x10^{-3}	1.9	Light Yellow	-
7	0.005	10x10^{-3}	1.9	Light Yellow	-
8	0.005	50x10^{-3}	1.9	Light Yellow	-

Table 2 Characteristics of PdNPs sol as a function of Cyclohexanone and 3- APTMS concentration.

S. No.	Cyclohexanone (mol dm^{-3})	Extent of PdNPs formation using 0.005 mol dm^{-3} K_2PdCl_4 and variable conc. of 3-APTMS (mol dm^{-3})		
		0.001x10^{-3}	0.01x10^{-3}	0.1x10^{-3}
1	0.3	+	+	---
2	0.6	+	+	---
3	0.9	+++	++	--
4	1.4	++++ (PdNP$_1$)	+++	+++ (PdNP$_3$)
5	1.9	++ (PdNP$_2$)	++++	++++ (PdNP$_4$)
6	2.4	-	-	++
7	2.8	-	-	-
8	3.2	-	-	-
9	3.5	-	-	-
10	3.8	-	-	-

3-APTMS and THF-HPO mediated synthesis of PdNPs, Pd-Au and Au-Pd. The synthesis of PdNPs[27] involves the mixing of the aqueous solutions of K_2PdCl_4 and 3-APTMS (1 M, 0.5 M and 0.25 M) under stirred conditions over a vertex cyclo mixer followed

by the addition of THF-HPO. The mixture turns into light black color within <15 min which subsequently converted to dark black color of PdNPs sol. The preparation of bimetallic nanoparticles involves both simultaneous and sequential reduction of known ratio of metal salts as reported earlier[27] with slight modification; Pd-Au is made using K_2PdCl_4 and $HAuCl_4$ in 4:1 ratio whereas Au-Pd is made using 1:4 ratios of the same. In simultaneous process for Pd-Au synthesis involves the mixing of 80 μL aqueous solution of K_2PdCl_4 (0.003 M) and 20 μL aqueous solution of $HAuCl_4$ (0.01 M) under stirred condition in 1 ml double distilled water followed by the addition of 10 μL of 3-APTMS (0.5 M) and 10 μL of THF-HPO (11.4 mg). The reaction mixture was turned into blackishred within 2 h. Whereas the Au-Pd under simultaneous process was made as follows: 80 μL aqueous solution of $HAuCl_4$ (0.01 M) was mixed with 20 μL aqueous solution of K_2PdCl_4 (0.003 M) under stirring condition in 1 ml double distilled water, followed by the addition of 10 μL of 3-APTMS (0.5 M) and 10 μL of THF-HPO (11.4 mg). After this, the colour of sol turned to reddish-black, indicating the formation of Au-Pd. In sequential method the synthesis of Pd-Au involves the mixing of 80 μl aqueous solution of K_2PdCl_4 (0.003 M) and 10 μl of 3-APTMS (0.5 M) followed by addition of

10 μl of THF-HPO (11.4 mg) under stirred condition in 1 ml double distilled water. The reaction mixture was turned to black color after 1 h. To this 20 μl of 3-APTMS capped $HAuCl_4$ (0.01 M) was added that enabled the formation of blackish-red color of Pd-Au within 2 h. Similarly, the sequential formation of Au-Pd involves the mixing of 80 μl aqueous solution of $HAuCl_4$ (0.01 M) and 10 μl of 3-APTMS (0.5 M) under stirred condition followed by the addition of 10 μl of THF-HPO (11.4 mg). The reaction mixture was turned to red color after 1 h which was followed by the addition of 20 μl of 3-APTMS capped K_2PdCl_4 resulting the formation of reddish-black colour of Au-Pd within 2 hr. All the synthesis was performed at room temperature.

Peroxidase-like catalytic activity of PdNPs. The peroxidase-like activity of as synthesized PdNPs were determined spectrophotometrically by measuring the formation of oxidized product of o-dianisidine at 430 nm (ε = 11.3 $mM^{-1}cm^{-1}$) using a Hitachi U-2900 spectrophotometer. Typically, the o-dianisidine oxidation activity was measured in water in the presence of as synthesized PdNPs (30 μl) using 30 μl of 20 mM o-dianisidine during 50 s at 25°C. PdNPs made at four compositions ($PdNP_1$, $PdNP_2$, $PdNP_3$ and $PdNP_4$) as shown in Table-2 were used for the

measurements. Hydrogen peroxide (30 µl, 30%) was added to start the reaction, unless otherwise specified.

Results and Discussion

Requirement of 3-APTMS during the synthesis of Pd nanoparticles

The role of organic amine has been demonstrated during the synthesis of gold and silver nanoparticles. It has been found that Au^{3+} or Ag^+ undergo specific interaction with 3-APTMS and controlled conversion of 3-APTMS capped metal ions into respective nanoparticles in the presence of suitable organic reducing agent is recorded.[19,28-30] Accordingly, at first instant, it is important to understand the interaction of 3-APTMS and palladium ions if any. Since 3-APTMS has two sites justifying its functional ability for said interaction, it is necessary to understand whether organic amine is playing the central role or alkoxysilane participate in such metal capping. Accordingly, we have studied interaction of K_2PdCl_4 with 3-APTMS or K_2PdCl_4 with tetraethoxyorthosilicate (TEOS) to resolve the issue. Fig.1(A, B) and 1(A', B') show the UV-Vis spectra and respective visual images justifying the interaction between Pd^{2+} ion and 3-APTMS (Fig. 1A, B) and Pd^{2+} ions with TEOS (Fig.1A', B'). The results clearly demonstrate capping of Pd^{2+} ions by organic amine.
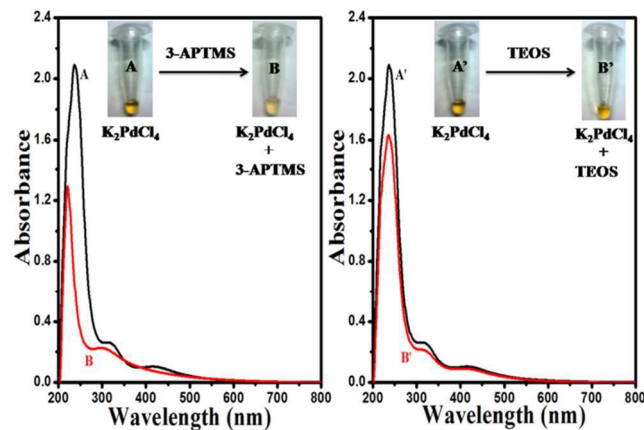

Fig. 1 Variation in the UV-Vis spectra of Methanolic solution of K_2PdCl_4 in absence and the presence of 3-APTMS (A, B) and TEOS (A', B') respectively.

It is now important to understand whether 3-APTMS capped palladium ions are only converted into respective nanoparticles through organic reducing agents or similar organic reducing agent may convert the palladium ions into respective nanoparticles in absence of 3-APTMS as well. Accordingly, Cyclohexanone / THF-HPO mediated synthesis of PdNPs has been investigated. Fortunately we found that THF-HPO alone is not efficient to convert Pd^{2+} ion into PdNPs in the absence of 3-APTMS however, cyclohexanone, even being a biphasic system, converts the same into PdNPs. Accordingly we have precisely investigated the synthesis of PdNPs justifying the role of 3-APTMS and organic reducing agent as discussed vide infra.

The results recorded in Fig.1(A, B) reveal that the presence of 3-APTMS in K_2PdCl_4 solution decrease in absorption close 420 nm which is characteristic of Pd^{2+} ions and reflect the possibility for the conversion of oxidation state

of the same. It has been recorded that cyclohexanone converts the Pd^{2+} ion into PdNPs in the absence of 3-APTMS. The finding reveals that 3-APTMS alone is not able to reduce Pd^{2+} ions into Pd^{0} whereas cyclohexanone efficiently convert the same into PdNPs both in absence and the presence of 3-APTMS. Accordingly a detailed investigation justifying the role of each component during the synthesis of PdNPs has been conducted. Fig. 2A shows SAED pattern of the PdNPs in absence of 3-APTMS while similar results in the presence of increasing concentrations of 3-APTMS ($0.001x10^{-3}$ and $0.1x10^{-3}$ M) are recorded in Fig. 2B and Fig. 2C respectively.
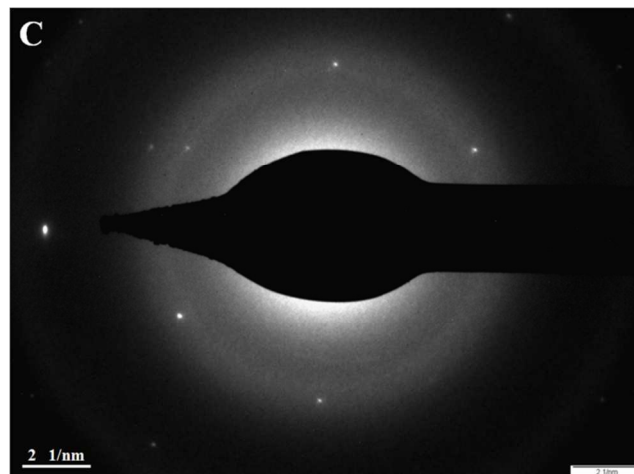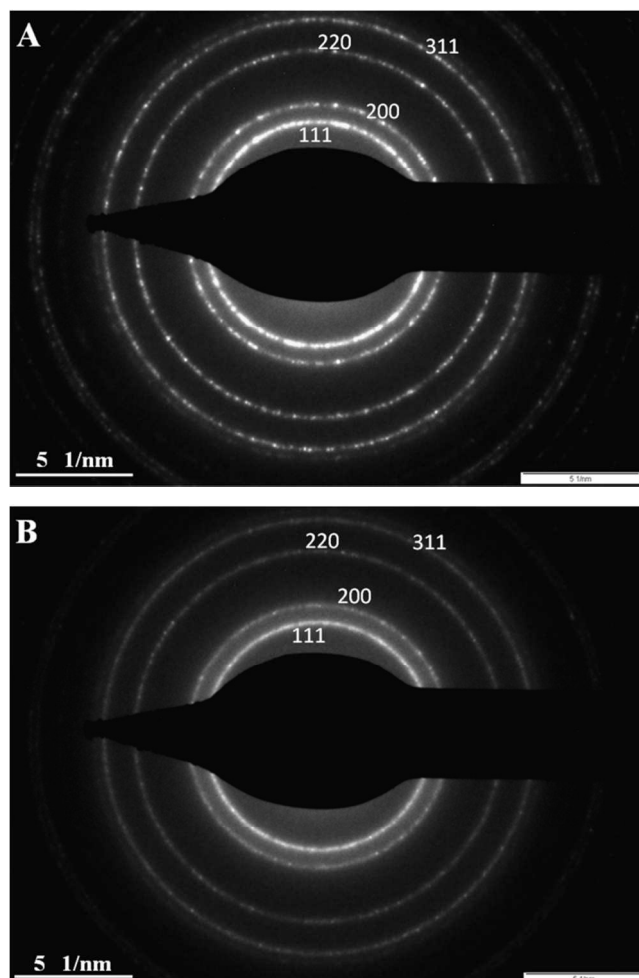

Fig. 2 SAED pattern of Palladium nanoparticles (PdNPs): (A) made by using 1.9 mol dm^{-3} cyclohexanone in absence of 3-APTMS; (B) and (C) made by using 1.9 mol dm^{-3} cyclohexanone with increasing concentrations of 3-APTMS ($0.001x10^{-3}$ mol dm^{-3} for B) and ($0.1x10^{-3}$ mol dm^{-3} for C).

In absence of 3-APTMS, PdNPs is polycrystalline in nature.[31-33] The electron diffraction pattern, as shown in Fig.2A, exhibited four sharp rings assigned to (111), (200), (220), and (311) lattice planes with spacing 0.224 nm (111), 0.192 nm (200) , 0.131 nm (220) of face centered cubic Pd. The results recorded on SAED patterns in the presence of increasing concentration of 3-APTMS ($0.001x10^{-3}$ to $0.1x10^{-3}$ M) reveal decreases in polycrystallinity of PdNPs as shown in Fig 2B and 2C respectively. The electron diffraction pattern, as shown in Fig.2B for PdNPs made with $0.001x10^{-3}$ M 3-APTMS, exhibited four diffused rings which again tend to diffused (Fig.2C) at $0.1x10^{-3}$ M 3-APTMS assigned again to Pd lattice. Decrease in polycrystallinity is also followed by remarkable changes in the morphology of nanomaterials as shown in Fig 3 A, B and C of

respective PdNPs. The inset of Fig. 3A, B and C shows the plot justifying the particle size distribution. The finding shows the average size of PdNPs close to 23.5 nm in the absence of 3-APTMS whereas 15 nm and 7 nm when 3-APTMS is 0.001×10^{-3}M, 0.1×10^{-3} M respectively. There is gradual increase in nanogeometry from Fig. 3A to C and justify the role of an organic amine in controlled synthesis of nanoparticles. The results recorded in Fig. 2 and Fig. 3 reveals following major observations; (a) decrease in polycrystallinity as a function of 3-APTMS concentrations, (b) an increase in nanogeometry of PdNPs with an increase in 3-APTMS
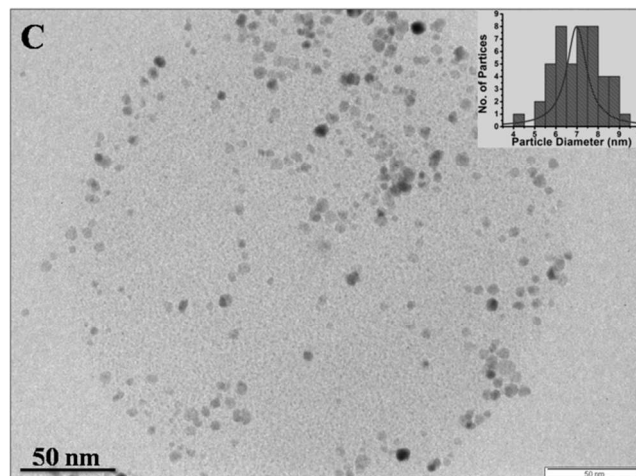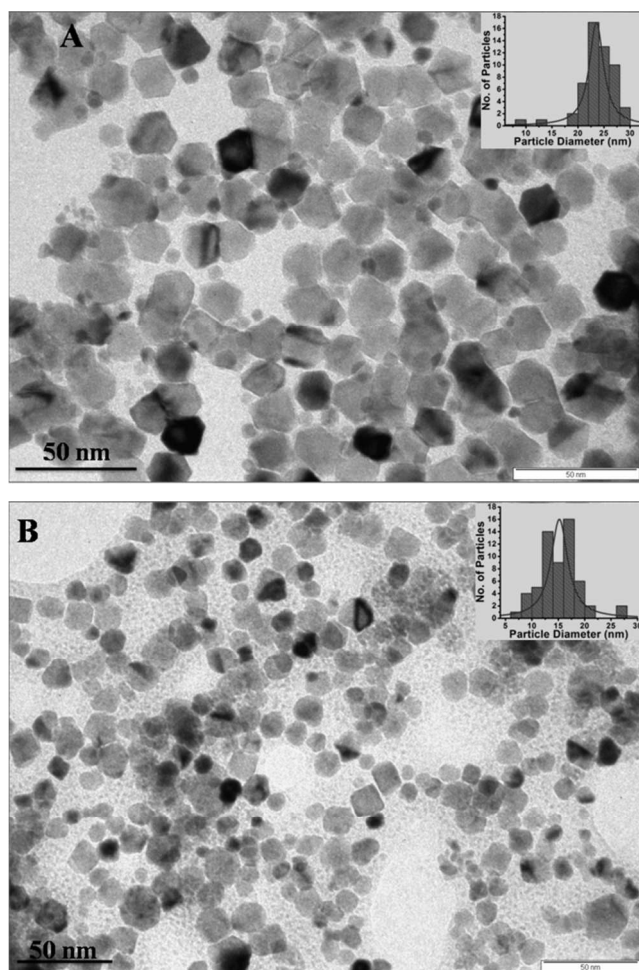

Fig. 3 TEM images of PdNPs made by using 1.9 mol dm^{-3} cyclohexanone (A) in absence and the presence of 0.001×10^{-3} mol dm^{-3} 3-APTMS (B) and 0.1×10^{-3} mol dm^{-3} 3-APTMS (C). Inset to Fig.3 shows the Particle size distribution.

concentrations, (c) transition of hexagonal geometry of PdNPs in absence of 3-APTMS into circular morphology in the presence of the same. Such variation in polycrystallinity and microstructure of PdNPs is found mainly due to interaction of silanol residue with as generated PdNPs made in the presence of 3-APTMS. Further insight on such interaction has been confirmed during the synthesis of bimetallic nanoparticles of Pd-Au and Au-Pd through simultaneous and sequential process of bimetallic nanoparticle synthesis as discussed videinfra.
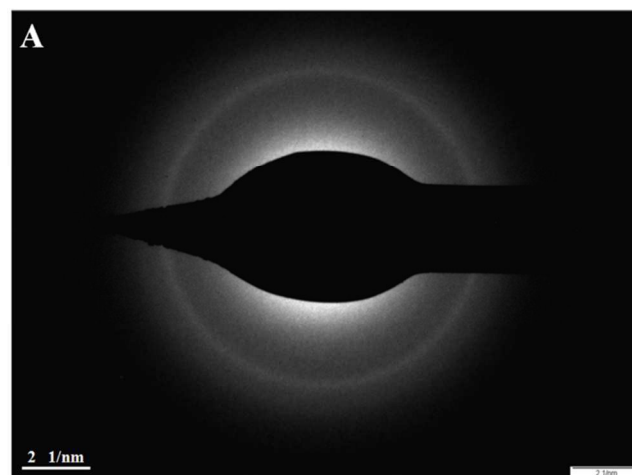
Requirement of 3-APTMS and an Organic reducing agent during the synthesis of bimetallic nanoparticles

The result as shown in Fig. 2 and 3 reveals the synthesis of PdNPs justifying the role of 3-APTMS and cyclohexanone. Since cyclohexanone even in absence of 3-APTMS

converts Pd^{2+} ion into PdNP, accordingly the choice of other reducing agent that allow the synthesis of the same only in the presence of 3-APTMS is sought for resolving the issues justifying the specific interaction of silanol residue with as generated PdNPs. THF-HPO has been found another organic reducing agent that precisely enables the synthesis of Pd, Pd-Au and Au-Pd nanoparticles in the presence of 3-APTMS only.[27] Therefore we investigated the SAED pattern and morphology of the Pd-Au and Au-Pd made through simultaneous and sequential process.

In order to resolve the issues justifying the specific interaction of silanol residue with as generated nanoparticles of two different ratio [(Pd^{2+} ions: 80%, Au^{3+} ions: 20 %) and [(Pd^{2+} ions: 20%, Au^{3+} ions: 80 %)] are allowed for bimetallic nanoparticles formation based on simultaneous and sequential process referred as Pd-Au and Au-Pd respectively. Fig. 4A and B shows SAED pattern of Pd-Au bimetallic nanoparticles synthesized by simultaneous and sequential process.[34,35] Similar results for Au-Pd are recorded as shown in Fig. 4C and D respectively. The results clearly demonstrate the occurrence of excellent polycrystalline pattern as shown in Fig. 4B and D when bimetallic nanoparticle formation takes place through sequential process. On the other hand simultaneous synthesis of the same (Pd-Au or Au-Pd) as shown in Fig. 4A and C enable decrease in polycrystallinity. The electron

diffraction pattern shows (111), (220) and (311). The lattice planes with spacing 0.235 nm, 0.139 nm and 0.122 nm of face centered cubic Pd-Au (Fig.4B). The results on Au-Pd (simultaneous) were indexed with the (111), (200) and (220) lattice planes with spacing 0.223 nm and 0.192 nm while pattern of Au-Pd (sequential) indexed with (220) and (311) lattice planes d-spacing 0.142 nm and 0.122 nm as shown in Fig. 4C and D respectively are recorded. Subsequently we investigated the morphology and size of as synthesized bimetallic nanoparticles. Fig. 5A, B, C and D respectively show the TEM images of the same made through simultaneous (Fig. 5A for Pd-Au and Fig. 5C for Au-Pd) and sequential (Fig. 5B for Pd-Au and Fig. 5D for Au-Pd) process. The average size of bimetallic Pd-Au and Au-Pd (Fig. 5A and 5C) are found to be 6.33 nm and 20.04 nm respectively, whereas the sizes of the same (Fig. 5B and 5D) are found to be 5.37 nm and 8.10 nm respectively.
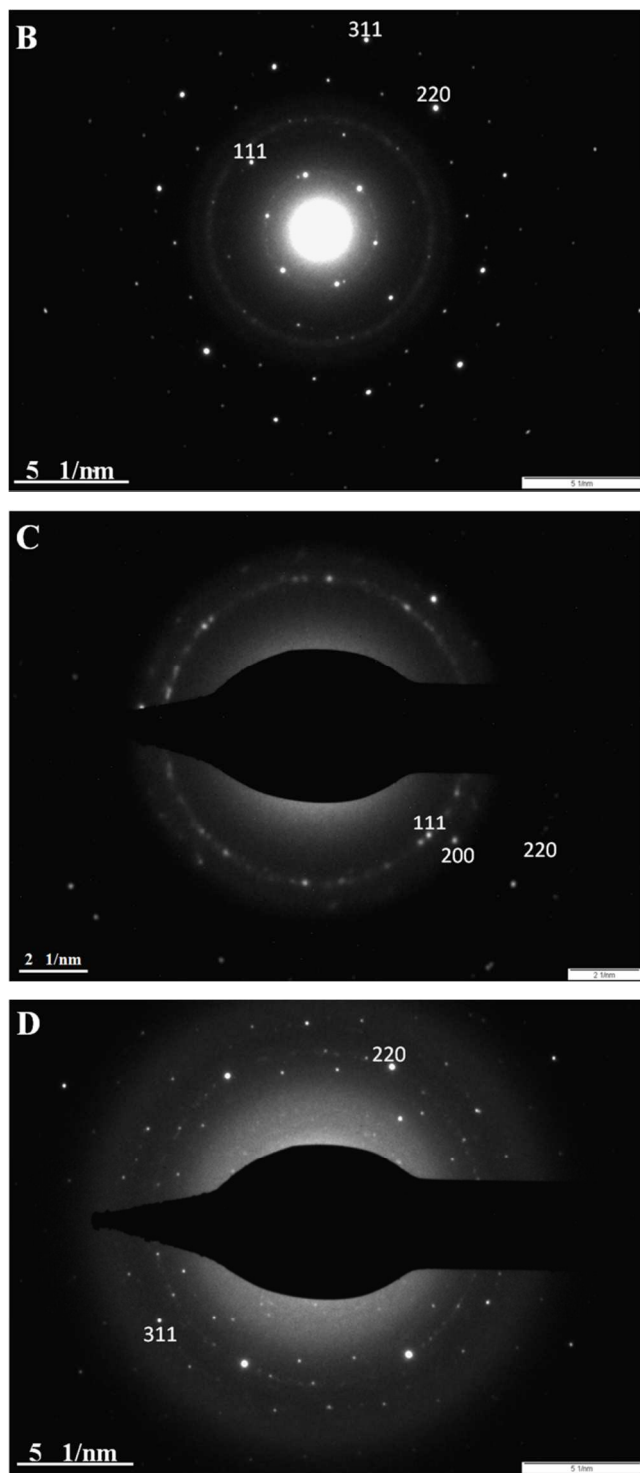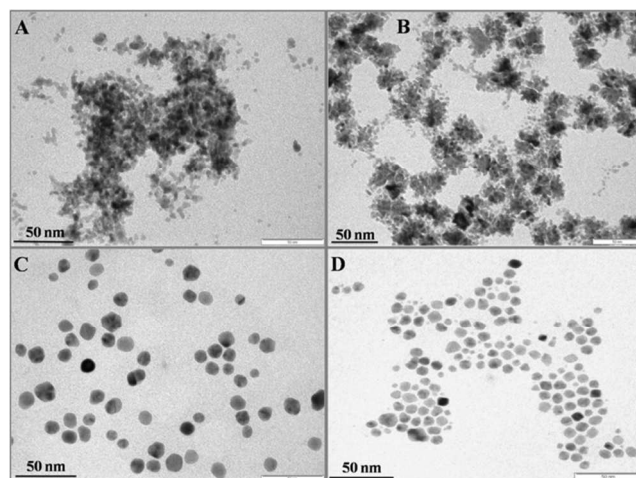
Fig. 5 TEM images of Pd-Au nanoparticles obtained
by simultaneous reduction of monometallic ions (A);
Pd-Au nanoparticles obtained by sequential reduction
of monometallic ions,(B); Au-Pd nanoparticles
obtained by simultaneous reduction of monometallic
ions (C) and Au-Pd nanoparticles obtained by
sequential reduction of monometallic ions (D). All
Bimetallic nanoparticles (Pd-Au/Au-Pd) were made
by using THF-HPO 11.4 mg and 0.5 mol dm^{-3} 3-
APTMS.

The results recorded in Fig.4 and 5 reveal
following major findings: (1) simultaneous
synthesis of bimetallic nanoparticles causes
decrease in polycrystalinilty; (2) when palladium
ions are reduced first, formation of bimetaliic
clusters is observed whereas initial reduction of
gold ions causes aggregation of same forming
larger nanoparticles. The aggregation on initial
reduction of gold ions during the formation of
bimetallic nanoparticles and bimetallic
nanoclusters has been reported by Toshima et
al.[36,37] However decrease in polycrystallinity
during simultaneous synthesis of bimetallic
nanoparticles need to be reviewed precisely.

***Effect of 3-APTMS on polycrystallinity and
morphology of PdNPs and bimetallic
nanoparticles.***

Fig. 4 SAED pattern of Pd-Au nanoparticles obtained
by simultaneous reduction of monometallic ions (A)
and by sequential reduction of monometallic ions (B);
obtained Au-Pd nanoparticles by simultaneous
reduction of monometallic ions (C) and obtained by
sequential reduction of monometallic ions (D). All
Bimetallic nanoparticles (Pd-Au/Au-Pd) were made
using 11.4 mg THF-HPO and 0.5 mol dm^{-3} 3-
APTMS.

The results shown in Fig.2 and Fig.4 reveal that as synthesised PdNPs has affinity for interaction with silanol moiety whereas AuNPs formed under similar conditions do not show such behaviour. Therefore simultaneous synthesis of PdNPs having more palladium contents results significant decrease in polycrystallinity as a function of silanol concentration (Fig.4A) whereas an increase in gold content under similar condition results relatively less decrease of the same (Fig.4C). Under sequential process of bimetallic nanoparticle synthesis when palladium is reduced first, formation of bimetallic nanoclusters takes place that restrict any further interaction with silanol moiety causing significant increase in polycrystallinity of the materials (Fig.4B).

It is again necessary to review the contribution of organic amine and silanol residues during nanoparticle synthesis. Our earlier findings[29,38] on the synthesis of AuNPs clearly demonstrate that an increase in 3-APTMS concentration causes decrease in nanogeometry e.g. increase in size whereas the results recorded in Fig.3 justify reverse results on PdNPs formation. The reasons for increase in size of AuNPs as a function of 3-APTMS concentration justified that the AuNPs are capped by organic amine residue increasing the hydrophilic behaviour of the same allowing the nanoparticle to come closer resulting aggregation of AuNPs with an increase in 3-APTMS concentration. However, as generated PdNPs has affinity for silanol residue enabling

an increase in hydrophobic components that restrict the aggregation of as generated PdNPs with significant change in morphology on increasing 3-APTMS concentration. Such finding is analogous to our earlier finding and support the transition in nanogeometry of nanomaterial in the presence of silica.[39]

Mechanism of 3-Aminopropyltrimethoxysilane and cyclohexanone mediated synthesis of PdNPs sol

In order to understand the mechanistic approach of PdNPs synthesis, it is necessary to justify the role of each components i.e. 3-APTMS and cyclohexanone enabling the formation of the same.
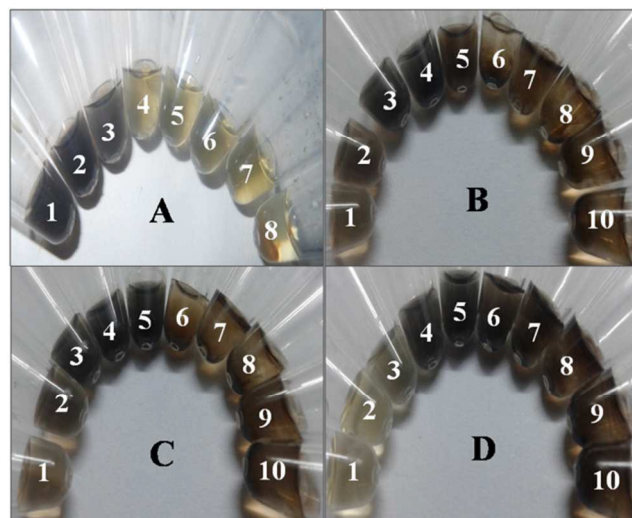

Fig. 6 (A) Effect of 3-APTMS concentrations ranging between 0.001×10^{-3} to 50×10^{-3} mol dm^{-3} (images 1-8) on the synthesis of PdNPs from 1.9 mol dm^{-3} cyclohexanone and 0.005 mol dm^{-3} K$_2$PdCl$_4$; (B) Effect of cyclohexanone concentrations ranging between 0.3 to 3.8 mol dm^{-3} (1-10) on the synthesis of PdNPs from 0.001×10^{-3} mol dm^{-3} 3-APTMS and 0.005 mol dm^{-3} K$_2$PdCl$_4$; (C) and (D) represent the similar results as that for of (B) at higher concentrations of 3-APTMS (0.01×10^{-3} mol dm^{-3} for C and 0.1×10^{-3} mol dm^{-3} for D) as shown in Table 2.

Accordingly we examined the formation of PdNPs under two different conditions; (1) keeping constant concentration of cyclohexanone while changing the concentration of 3-APTMS; and (2) keeping 3-APTMS constant while changing the concentrations of cyclohexanone. Fig. 6A shows the visual photographs of PdNPs made from the use of 0.005 M K_2PdCl_4, 1.9 M cyclohexanone and variable concentration of 3-APTMS ranging between 0.001×10^{-3} to 50×10^{-3} M as shown in Table 1. Under this condition only three concentration of 3-APTMS (0.001×10^{-3}, 0.01×10^{-3} and 0.1×10^{-3} M enable the formation of PdNPs sol (1, 2 and 3) as shown in Fig.6A and Table 1. These three concentrations of 3-APTMS were then allowed to investigate the effect of cyclohexanone on the synthesis of PdNPs. The findings as shown in Fig 6B, C and D justify the requirement of optimum concentrations of cyclohexanone as a function of 3-APTMS concentrations. Both lower and higher concentration beyond the optimum concentration does not enable the formation of PdNPs (Table 2, Fig.6B, C and D). Higher concentration of cyclohexanone results into a biphasic system. The proposed mechanism for the 3-APTMS and cyclohexanone mediated synthesis is shown in scheme-1:
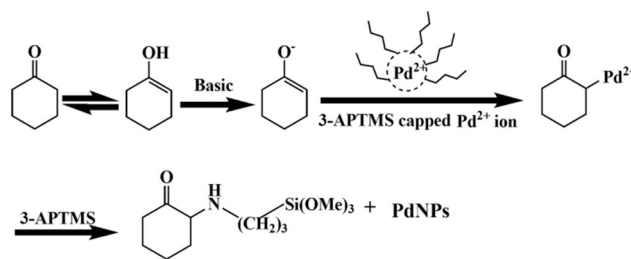
Scheme. 1 Mechanism of 3-APTMS and Cyclohexanone assisted synthesis of PdNPs.

Cyclohexanone in the prevailing medium undergoes keto-enol tautomerism. Enolate ion acts as an electron donor to 3-APTMS capped Pd^{2+} ion, which in turn acts as a lewis acid, leading to the formation of PdNPs.

Effect of 3-APTMS and organic reducing agents on the dispersibility of PdNPS

Dispersibility of PdNPs largely depends on the medium which in turn is determined by the apparent polar or nonpolar behaviour of the organic moieties (THF-HPO/Cyclohexanone). First we discuss the Dispersibility of PdNPs made using 3-APTMS and cyclohexanone both in aqueous and organic solvents viz. Water, Methanol, Acetonitrile and Toluene. It is important to understand the dispersibility of as synthesized PdNPs in aqueous and non-aqueous solvents. Fig. 7A, B and C shows the dispersibility of as synthesized PdNPs in water, methanol, acetonitrile and toluene. PdNPs is found dispersible in water, methanol and acetonitrile while non-dispersible or insoluble in toluene. The data as shown in Table 3 justify that the PdNPs shows better dispersibility in water, methanol and acetonitrile while not dispersible in toluene. However, PdNPs made using 3-APTMS

and THF-HPO are dispersible in both aqueous and organic solvents viz. Water, Methanol, Acetonitrile and Toluene.
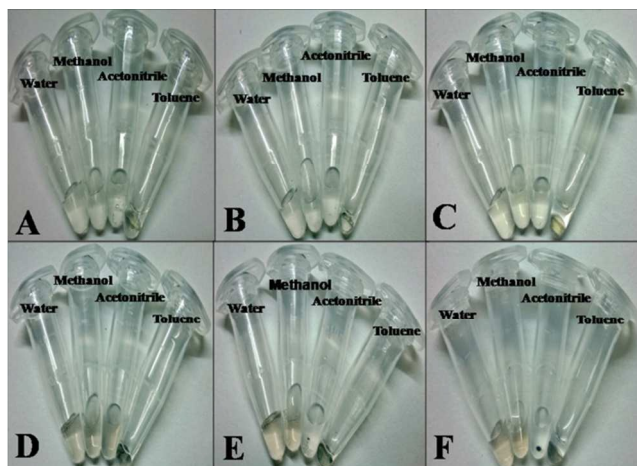

Fig.7 Visual photographs of PdNPs made by using composition of 3-APTMS, Cyclohexanone and K_2PdCl_4 as shown in Table 3 (A, B and C) and their dispersibility in water, methanol, acetonitrile and toluene. Visual photographs of PdNPs made by using 3-APTMS, THF-HPO and K_2PdCl_4 as shown in Table 3 (D, E and F) and their dispersibility in water, methanol, acetonitrile and toluene.

Fig. 7D, E and F shows the dispersibility of as synthesized PdNPs in water, methanol, acetonitrile and toluene. The data as shown in Table 3 justify that the PdNPs shows better dispersibility in water and methanol at all composition that enable the formation of PdNPs. However the dispersbility in acetonitrile is found to be function of 3-APTMS concentration. Higher concentration of 3-APTMS (1.0M and 0.5 M) restricts dispersbility in acetonitrile whereas PdNPs made at lower concentrations of the same are dispersible in this solvent. The reasons for the variation in dispersibity of PdNPs are due the micellar behaviour of 3-APTMS and

CMC of organic reducing agent.

Table 3 Dispersibility of PdNPs in water, methanol, acetonitrile and toluene made by using varying concentrations of 3-APTMS and constant concentrations of Cyclohexanone/THF-HPO. "+" and "-" sign denotes increasing and decreasing extent of PdNPs dispersibility in the same.

S. No.	3-APTMS (mol dm⁻³)	Name of Organic Reducing Agent		Relative Dispersibility of PdNPs in Various Solvents			
		Cyclohexanone (mol dm⁻³)	THF-HPO (mg)	Water	Methanol	Acetonitrile	Toluene
A	0.001×10^{-3}	1.9	-	++++	++++	++++	----
B	0.01×10^{-3}	1.9	-	++++	++++	++++	----
C	0.1×10^{-3}	1.9	-	++++	++++	++++	----
D	0.25	-	11.4	++++	++++	++++	----
E	0.5	-	11.4	++++	++++	--	----
F	1	-	11.4	++++	++++	---	----

Functional application of PdNPs as Peroxidase mimetic. Generally, Peroxidase enzyme, H_2O_2 and color substrate based systems are typically employed for routine applications in ELISA kits and other bioassay. The activity of peroxidase in such kit remains in question due to least stability of the same for practical applications. These disadvantages have directed for investigating enzyme mimetics. Recently, it has been reported that many nanomaterials, such as noble metal nanoparticles, metal oxide, Prussian blue and their composites possess intrinsic peroxidase-like activity and have proclaimed their use as peroxidase replacement.[40-42]
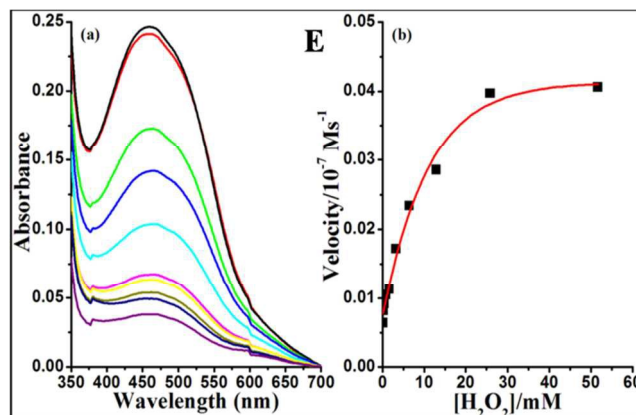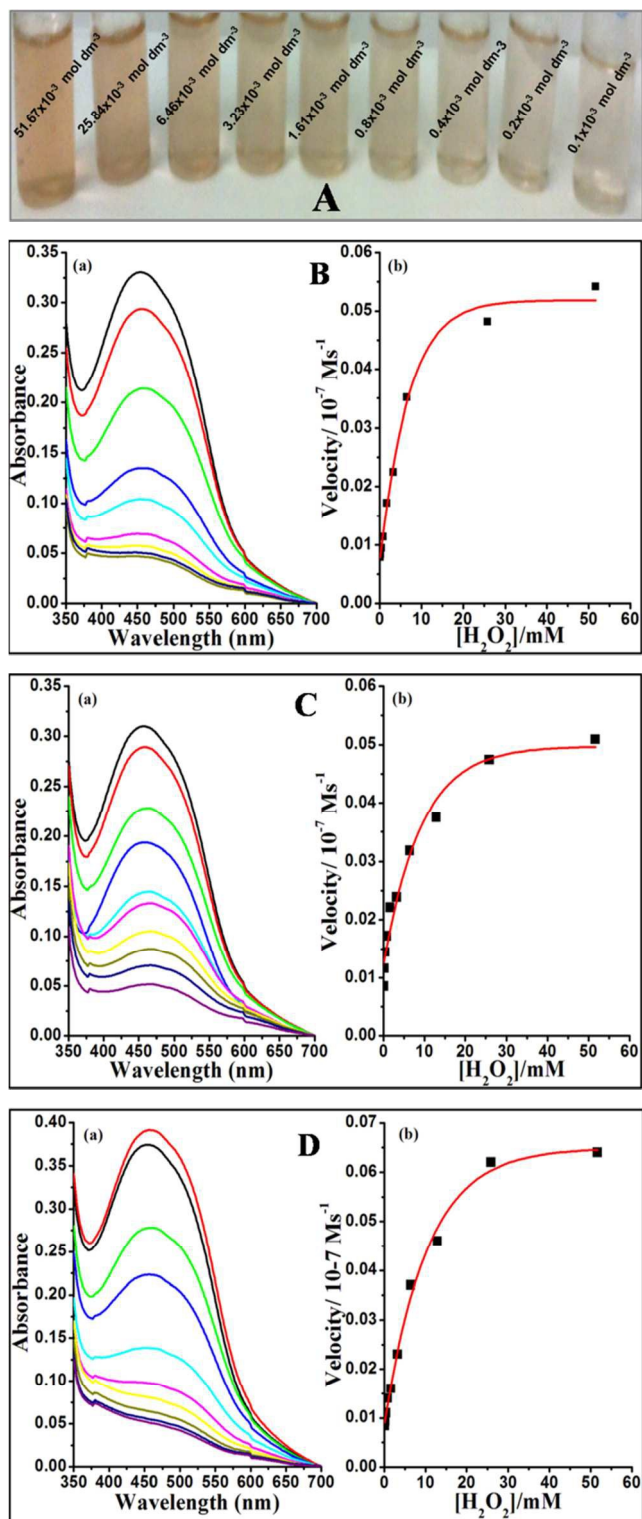
Fig. 8 (A) A typical photograph showing colour evaluation upon addition of o-dianisidine by varying concentrations of H_2O_2 and constant PdNPs. (B-a,), (C-a,), (D-a,) and (E-a,) represent the UV-Vis spectra of o-dianisidine oxidation products on the addition of PdNP$_1$, PdNP$_2$, PdNP$_3$, PdNP$_4$ with various concentrations of H_2O_2 (0.1, 0.2, 0.4, 0.8, 1.61, 3.23, 6.46, 25.84, 51.67x10^{-3} mol dm^{-3}); (B-b), (C-b,), (D-b,) and (E-b,) shows steady-state kinetic assay of the same.

PdNPs, due to sufficient stability and biocompatibility and possibility of its synthesis at the time of application make a potential candidate of peroxidase mimetic. Accordingly, attempt has been made to evaluate the peroxidase mimetic ability of as-synthesized PdNPs as a function of 3-APTMS and cyclohexanone concentrations. Fig. 8 shows the catalytic property of PdNPs (PdNP$_1$, PdNP$_2$, PdNP$_3$, and PdNP$_4$ as shown in Table 2) made with increasing concentrations of 3-APTMS and cyclohexanone on the oxidation of o-dianisidine-H_2O_2 system. The K_m value of PdNPs increases with increase in 3-APTMS concentrations as shown in Table 4. At lower concentration of 3-APTMS and cyclohexanone, K_m value is found close to 3.6 mM. Such a low K_m value recorded using feasible amount of

PdNPs when compared with HRP catalyzed reaction (3.7 mM) involving possible amount of active protein to exploit during routine laboratory direct the use of as synthesized nanoparticles in technological evolution.

Table 4 Kinetic parameters for the peroxidase-like activity of PdNPs.

S. No	System	K_m/mM	V_{max}/ms^{-1}
A	PdNP$_1$	3.6	0.051x10^{-7}
B	PdNP$_2$	4.0	0.049x10^{-7}
C	PdNP$_3$	4.8	0.064x10^{-7}
D	PdNP$_4$	5.3	0.041x10^{-7}

We have also examined the advantages of the present process for the synthesis of PdNPs and bimetallic nanoparticles from that of those reported earlier[1,4,36,37,43-45]. Nanoparticles reported earlier require suitable functionality for anchoring the targeted ligand for specific applications. In addition to that these nanoparticles do not show functional ability and are not dispersible in variety of polar and non-polar solvents under normal conditions. The as synthesized nanoparticles reported herein possess organic amine as potential functionality for meeting these requirements.

Conclusions

Controlled conversion of Pd^{2+} ions into PdNPs involving active role of 3-APTMS and organic reducing agents are reported. The

Polycrystallinity and nanogeometry of PdNPs are found as a function of 3-APTMS concentration. Such variation in polycrystallinity and microstructure of PdNPs is found mainly due to interaction of silanol residue with as generated PdNPs made in the presence of 3-APTMS. The results on bimetallic Pd-Au or Au-Pd also justify potential affinity of PdNPs with silanol whereas AuNPs do not show such affinity. When palladium ions are reduced first, formation of bimetallic clusters is observed whereas initial reduction of gold ions causes aggregation of same forming larger nanoparticles. Formation of bimetallic nanoclusters tend to decrease the silanol interaction justifying an increase in polycrystallinity as compared to that of the same under simultaneous synthesis of bimetallic nanoparticles. The as generated palladium nanoparticles show excellent peroxidise mimetic ability with K_m value to the order of 3.6 mM indicating complete replacement of HRP used in biomedical application.

Acknowledgements

Notes and references

1   Y. Niu, L. K. Yeung and R. M. Crooks, *J. Am. Chem. Soc.*, 2001, **123**, 6840-6846.

2   J. Huang, T. Jiang, B. Han, H. Gao, Y. Chang, G. Zhao and W. Wu, *Chem. Commun.*, 2003, 1654-

1655.

3   N. Semagina, A. Renken and L. Kiwi-Minsker, *J. Phys. Chem. C,* 2007,**111**, 13933-13937.

4   O. M. Wilson, M. R. Knecht, J. C. Garcia-Martinez and R. M. Crooks, *J. Am. Chem. Soc.*, 2006, **128**,4510-4511.

5   H. P. Hemantha and V. V. Sureshbabu, *Org. Biomol. Chem.*, 2011, **9**, 2597-2601.

6   N. Dimitratos, F. Porta and L. Prati, *Appl. Catal. A: Gen.*, 2005, **291**, 210-214.

7   Z. Hou, N. Theyssen, A. Brinkmann and W. Leitner, *Angew. Chem. Int. Ed.*, 2005, **44**, 1346-1349.

8   B. Karimi, S. Abedi, J. H. Clark and V. Budarin, *Angew. Chem. Int. Ed.,* 2006, **45**, 4776-4779.

9   Q. Liang, J. Liu, Y. Wei, Z. Zhao and M. J. MacLachlan, *Chem. Commun.*, 2013, **49**, 8928-8930.

10   M. Beller, H. Fischer, K. Kuhlein, C. P. Reisinger and W. A. Hermann, *J. Organomet. Chem.,* 1996, **520**, 257-259.

11   R. Narayanan and M. A. El-Sayed, *J. Catal.,* 2005, **234**, 348-355.

12   S. Cheong, J. D. Watt and R. D. Tilley, *Nanoscale*, 2010, **2**, 2045-2053.

13   C. Bianchini and P. K. Shen, *Chem. Rev.*, 2009, **109**, 4183-4206.

14   A. Saez, J. S. Gullon, E. Exposito, A. Aldaz and V. Montiel, *Int. J. Electrochem. Sci.,* 2013, **8**, 7030-7043.

15   N. V. Long, C. M. Thi, Y. Yong, M. Nogami and M. Ohtaki, *J. Nanosci. Nanotechnol.,* 2013, **13**, 4799-4824.

16   C. Xu, K. Xu, H. Gu, X. Zhong, Z. Guo, R. Zheng, X. Zhang and B. Xu, *J. Am. Chem. Soc.*, 2004, **126**, 3392-3393.

17   T. Mirzabekov, H. Kontos, M. Farzan, W. Marasco and J. Sodroski, *Nat Biotechnol.*, 2000, **18**, 649-654.

18   K.Saha, S.S.Agasti, C. Kim, X. Li and V. M. Rotello, *Chem. Rev.*, 2012, **112**, 2739-2779.

19   P. C. Pandey and D. S. Chauhan, *Analyst*, 2011, **137**, 376-385.

20   P. C. Pandey, S. Upadhyay and H. C. Pathak, *Electroanalysis*, 1999, **11**, 59-65.

21   P. C. Pandey, S. Upadhyay, V. S. Tripathi and I. Tiwari, *Electroanalysis*, 1999, **11**, 1251-1258.

22   P. C. Pandey and S. Upadhyay, *Sens. Actuators. B*, 2001, **78**, 148-155.

23   P. C. Pandey, S. Upadhyay and H. C. Pathak, *Electroanalysis*, 1999, **11**, 950-958.

24   P. C. Pandey, S. Upadhyay, I. Tiwari and S. Sharma, *Electroanalysis*, 2001, **13**, 1519-1527.

25   P. C. Pandey, S. Upadhyay, N. K. Shukla and S. Sharma, *Biosens & Bioelect.*, 2003, **18**, 1257-1268.

26   P. C. Pandey and B. C. Upadhyay, *Molecules*, 2005, **10**, 728-739.

27   P. C. Pandey, R. Singh and A. K. Pandey, *Electochim. Acta*, 2014, **138**, 163-173.

28   P. C. Pandey, A. K. Pandey and G. Pandey, *J. Nanosci. Nanotechnol.*, 2014, **14**, 6606-6613.

29   P. C. Pandey and G. Pandey, *J. Mater. Chem. B*, 2014, **2**, 3383-3390.

30   P. C. Pandey and R. Singh, *J. Nanosci. Nanotechnol.*, 2015, **15**, 5749-5759.

31   P. Bayliss, D. C. Erd, M. E. Mrose, A. P. Sabina and D. K. Smith, *Mineral Powder Diffraction File-Data Book-JCPDS.*, 1986.

32   U. Schlotterbeck, C. Aymonier, R. Thomann, H. Hofmeister, M. Tromp, W. Richtering and S. Mecking, *Adv. Funct. Mater.*, 2004, **14**, 999-1004.

33   S. W. Kim, J. Park, Y. Jang, Y. Chung, S. Hwang and T. Hyeon, *Nano Lett.*., 2003, **3**, 1289-1291.

34   R. Harpeness and A. Gedanken, *Langmuir*, 2004, **20**, 3431-3434.

35   F. Ksar, L. Ramos, B. Keita, L. Nadjo, P. Beaunier and H. Remita, *Chem. Mater.*, 2009, **21**, 3677-3683.

36   M. Harada, K. Asakura and N. Toshima, *J. Phys. Chem.*, 1993, **97**, 5103-5114.

37   N. Toshima and T. Yonezawa, *New J. Chem.*, 1998, 1179-1201.

38   P. C. Pandey, D. Pandey and G. Pandey, *RSC Advances.*, 2014, **4**, 60563-60572.

39   P. C. Pandey and A. Prakash, *Electroanalysis*, 2011, **23**, 1991-1997.

40   H. Chen, Y. Li, F. Zhang, G. Zhang and X. Fan, *J. Mater. Chem.,* 2011, **21**, 17658-17661.

41   P. C. Pandey and A. K. Pandey, *Analyst*, 2013, **138**, 2295-2301.

RSC Advances Accepted Manuscript

42   P. C. Pandey and A. K. Pandey, *Electochim. Acta*, 2013, **109**, 536-545.

43   M. Zhao, K. Deng, L. He, Y. Liu, G. L. Zhao and Z. Tang, *J. Am. Chem. Soc*., 2014, **136**, 1738-1741.

44   M. R. Knecht, M. G. Weir, A. I. Frenkel and R. M. Crooks, *Chem. Mater*., 2008, **20**, 1019-1028.

45   B. Xia, F. He and L. Li, *Langmuir*, 2013, **29**, 4901-4907.

5

10